

Interactions between a surface active imidazolium ionic liquid and BSA

Fei Geng · Liqiang Zheng · Jie Liu · Li Yu ·
Chenho Tung

Received: 23 March 2009 / Revised: 24 June 2009 / Accepted: 21 July 2009 / Published online: 5 August 2009
© Springer-Verlag 2009

Abstract The interactions between a surface active imidazolium ionic liquid (IL), 1-tetradecyl-3-methylimidazolium bromide ($C_{14}\text{mimBr}$) and bovine serum albumin (BSA) were studied. To investigate the structure changes of BSA induced by addition of $C_{14}\text{mimBr}$, this system was studied by surface tension, isothermal titration microcalorimetry, far-UV circular dichroism (CD) and fluorescence spectra. The surface tension measurement shows the formation of $C_{14}\text{mimBr}$ /BSA complex and the effect of the complex on surface tension. Furthermore, it reveals the interaction type. The enthalpy change in the whole interaction process between $C_{14}\text{mimBr}$ and BSA was obtained by isothermal titration microcalorimetry, and the results prove the alteration of the BSA structure. To realize the structure alteration position more definitely, far-UV CD was used to obtain the contents of α -helix and random coil. Changes of these contents reveal that the secondary structure of BSA changes with addition of $C_{14}\text{mimBr}$. Fluorescence spectra are used to prove that the alteration of the secondary structure is due to the interactions of $C_{14}\text{mimBr}$ molecules and amino acid residues. They show that tryptophan (Trp)

residues, one of the intrinsic fluorophores in BSA, are exposed to a hydrophobic microenvironment with the addition of $C_{14}\text{mimBr}$.

Keywords Surface active imidazolium ionic liquid · Bovine serum albumin · Interaction · Structure alteration

Introduction

Knowledge of interactions between surfactants and proteins is helpful to understand the action of surfactants as solubilizing agents and denaturants for proteins. When a surfactant binds to a protein, the intramolecular forces which maintain the secondary structure of the protein are altered, producing conformational changes in the protein [1]. These conformational changes often lead to changes of the polarity and functional properties of the proteins [2]. The interactions may be advantageous and may stabilize the proteins or they may decrease the protein stability [3–5]. The effect of surfactant on protein depends on the characteristics of both surfactant and protein. Besides, surfactant concentrations and environmental conditions also affect the interactions.

Quantitative thermodynamic parameters accompanying the thermal denaturation of globular proteins in the presence of nonionic surfactant TX-100 were determined by isothermal titration calorimetry and differential scanning calorimetry [1]. TX-100 can bind to proteins in monomer and micelle forms and the stoichiometry for both cases is 4:1. Interactions of bovine serum albumin (BSA) with a gemini cationic surfactant and a common cationic surfactant were compared by isothermal titration calorimetry [5]. The gemini surfactant binds to BSA more strongly than the ordinary surfactant. Interactions of BSA with cationic and

F. Geng · L. Zheng · L. Yu (✉)
Key Laboratory of Colloid and Interface Chemistry,
Shandong University,
Ministry of Education,
Jinan 250100, People's Republic of China
e-mail: ylmlt@sdu.edu.cn

J. Liu
Department of Chemistry, Liaocheng University,
Liaocheng 252059, People's Republic of China

C. Tung
Technical Institute of Physics and Chemistry,
Chinese Academy of Sciences,
Beijing 100190, People's Republic of China

anionic surfactant mixtures have been studied by isothermal titration calorimetry and differential scanning calorimetry [6]. Addition of a high concentration of cationic surfactant produced an insoluble surfactant/BSA complex but addition of an anionic surfactant did not. Isothermal titration calorimetry is a powerful technique to study interactions of surfactants and proteins. It can directly determine the interaction enthalpy when surfactant molecules are added to protein molecules [7]. In addition, surface tension, potentiometry, dynamic light scattering, and small angle neutron scattering are commonly used to investigate the interactions between surfactants and proteins [8–11].

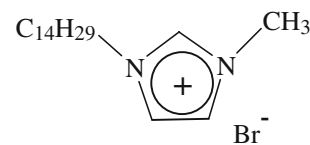
BSA is selected as a model globular protein, because its structure and physicochemical properties are well characterized [6]. It has well-established secondary structure, stability, water solubility, and versatile-binding capacity [12–14]. BSA can bind many different types of amphiphilic biological molecules, which are believed to play an important role in determining the physiological function [15]. Surface active imidazolium ILs and conventional cationic surfactant, alkyltrimethylammonium bromide, are similar in amphiphilic molecular structure. Previous work in our group indicated that the CMC of surface active imidazolium ILs in aqueous solution is lower than that of alkyltrimethylammonium bromide which demonstrates that the surface activity of surface active imidazolium ILs is superior to that of alkyltrimethylammonium bromide [16]. To investigate whether the surface active imidazolium ILs can bind to protein just as alkyltrimethylammonium bromide interacts with protein can extend new application of surface active imidazolium ILs. $C_n\text{mimBr}$ ($n=10, 12, 14,$ and 16) is a cross-sectional series of surface active imidazolium ILs. The solubility of $C_{16}\text{mimBr}$ in water is not good. The surface activity of $C_{10}\text{mimBr}$ and $C_{12}\text{mimBr}$ is lower than that of $C_{14}\text{mimBr}$. Considering the good solubility and excellent surface activity of $C_{14}\text{mimBr}$, it was chosen as the object of study in this work. The effect of $C_{14}\text{mimBr}$ on BSA structure and the influence of the structure changes on BSA stability and activity are described in this paper.

Materials and methods

Materials

BSA was purchased from Amresco with a sharp molecular weight distribution at 6.6×10^4 g/mol. Surface active imidazolium IL, $C_{14}\text{mimBr}$ (Fig. 1), was synthesized as described in reference [16]. The purity of the sample was checked by $^1\text{H-NMR}$ spectroscopy. TTAB (A. R.) was purchased from Shanghai Chemical Co. and was recrystallized twice from anhydrous alcohol. Triply distilled water

Fig. 1 Chemical structure of 1-tetradecyl-3-methylimidazolium bromide, $C_{14}\text{mimBr}$



was used for all the experiments. The pH values of the solutions before and after the experiments were in the range from 6.5 to 7.0. It should be noted that, since the isoelectric point of BSA occurs at 4.9, under these conditions, it is negatively charged.

Surface tension

Surface tension measurements were carried out on a Krüss K12 tensiometer (Switzerland, accuracy ± 0.01 mN/m) using the ring method. Temperature was controlled with an HAAKE DC 30 thermostatic bath (Switzerland, accuracy ± 0.1 °C). The surface tension was determined by single measurements. All measurements were repeated at least three times. The values of CMC and surface tension at the CMC (γ_{CMC}) were determined from the intersection of the two lines drawn in low- and high-concentration regions in surface tension via concentration curves using a linear regression analysis method [17]. The experiments were carried out at 25, 35, and 45 °C.

Isothermal titration microcalorimetry

A 2277 TAM isothermal titration microcalorimeter (Thermometric, Sweden) controlled by Digitam 4.1 software was used for direct measuring of enthalpy. As comparison, TTAB was added into 5×10^{-5} mol/L BSA. The 1 mL reaction and reference cell made from stainless steel were initially loaded with 0.50- and 0.74-mL BSA solution, respectively. A 500- μL injection syringe was used for all studies. Titration concentrations of $C_{14}\text{mimBr}$ and TTAB were chosen to be approximately five times of the CMC: 1.3×10^{-2} and 2.0×10^{-2} mol/L, respectively. Injections of 24×12 - μL surfactant solution were made into the reaction vessel with a 4-min interval between each injection. To ensure stability, the samples were stirred at 30 rpm. The error of the experimental results is $\pm 0.3\%$. The experiments were carried out at 25 °C.

Far-UV Circular Dichroism spectra

Far-UV dichroism (CD) spectra were obtained with a Jasco J-810 spectropolarimeter, using a bandwidth of 2.0 nm and a cell of 0.1 mm path length over the wavelength range from 190 to 260 nm. The α -helix structure in BSA presents double minima at 208 and 222 nm. The minimum at 215 nm suggests the existence of β -sheet structure [18].

The spectropolarimeter was purged sufficiently with pure nitrogen before starting the instrument. Each spectrum was baseline-corrected, and the final plot was taken as an average of three accumulated plots. The α -helical, β -sheet, β -turn and random coil contents were analyzed by using the curve fitting method of the Jasco secondary structure manager. The experiments were carried out at 25 °C.

Fluorescence spectra

Fluorescence spectra were carried out on a Hitachi F-4500 fluorescence spectrophotometer using a 1.0 cm quartz cell. The excitation spectra of BSA studied in this work was 280 nm. Synchronous fluorescence spectra were acquired by the same spectrofluorometer. The spectra were recorded, keeping the difference between excitation wavelength and emission wavelength fixed ($\Delta\lambda = \lambda_{em} - \lambda_{ex}$). When $\Delta\lambda$ is 20 or 60 nm, the synchronous fluorescence spectra give characteristic information about tyrosine (Tyr) residues or tryptophan (Trp) residues [19, 20]. All the excitation and emission slits were set at 10/2.5 nm. The experiments were carried out at 25 °C.

Results and discussion

Surface tension measurement

Surface tension measurement is a simple and effective method to prove the interaction between macromolecules and surfactants. Figure 2 presents the surface tension curves of C_{14} mimBr/BSA systems at different temperatures. The first break points occur when the concentration of C_{14} mimBr is 1×10^{-6} mol/L, corresponding to the initial formation of C_{14} mimBr/BSA complexes, where the concentration is known as the critical aggregation concentration (CAC) [21]. It is valuable to note that the CAC values are independent of BSA concentrations and are only dependent on the characteristics of the surfactant. When the concentration of C_{14} mimBr is somewhat above the CAC, the increasing surfactant molecules almost all combine with BSA. Therefore, no more surfactant molecules appear at the air/water interface, and the surface tension curves exhibit a short plateau. It is found from Fig. 2 that temperature has no effect on CAC values. Because electrostatic attraction is affected only weakly by temperature, this result indicates that C_{14} mimBr binds to BSA through electrostatic attractions at concentrations near the CAC [22]. When the concentration of C_{14} mimBr is above 1×10^{-3} mol/L, a second break point appears which corresponds to the CMC of C_{14} mimBr aqueous solution in the presence of BSA. The CMC values are listed in Table 1. The CMCs increase with the increment of BSA because

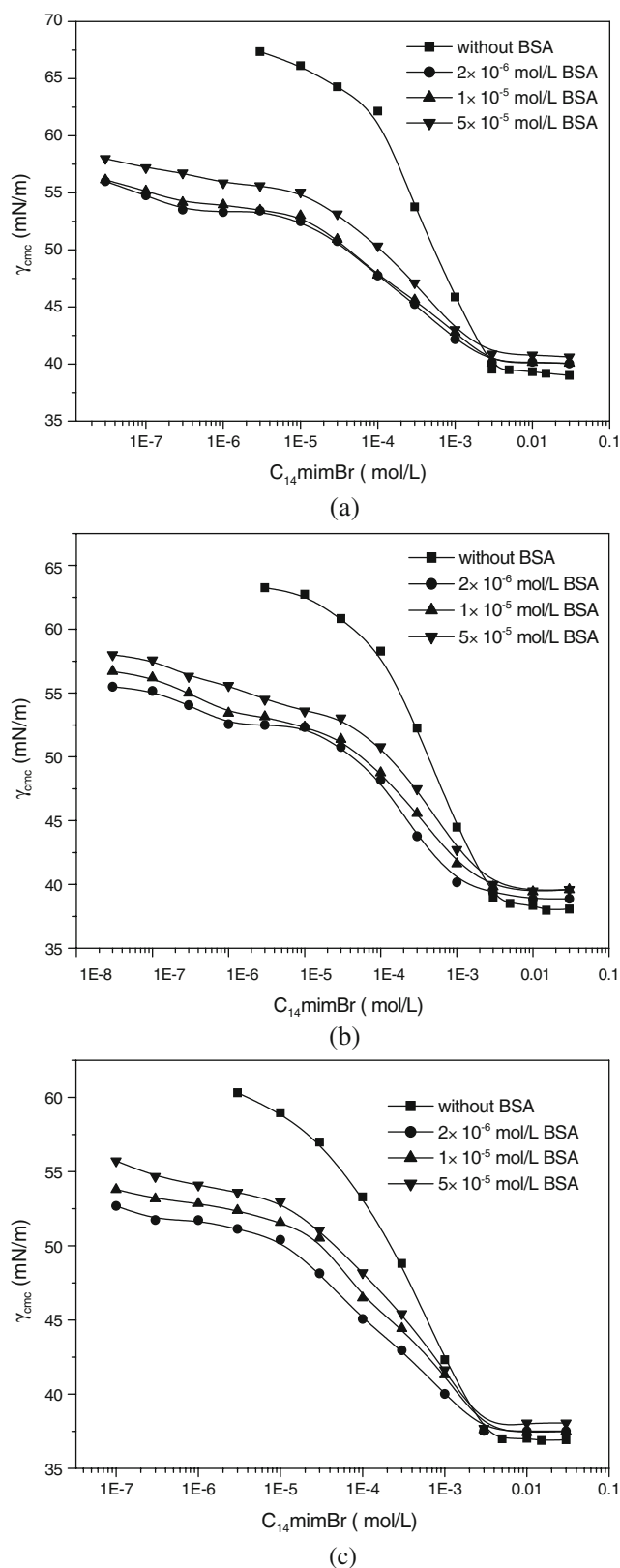


Fig. 2 Surface tension of C_{14} mimBr/BSA at various temperatures. **a** 25 °C. **b** 35 °C. **c** 45 °C

Table 1 CMC values of C_{14} mimBr/BSA at various temperatures

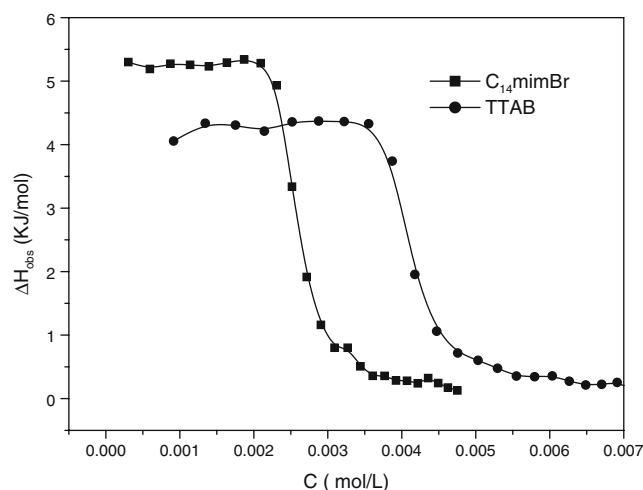
Concentration of BSA (mol/L)	CMC ($\times 10^{-3}$ mol/L)		
	25°C	35°C	45°C
0	2.76	2.85	3.17
2×10^{-6}	2.94	2.95	3.20
1×10^{-5}	3.11	3.08	3.36
5×10^{-5}	3.26	3.55	3.81

C_{14} mimBr molecules combine with BSA before micellization. Table 1 also shows that the CMC values increase with increasing temperature when the BSA concentration is fixed. More C_{14} mimBr monomers dissolve at higher temperature, which inhibits micellization [22]. Additionally, the increasing temperature promotes the thermal motion of surfactant molecules and the molecules are more likely to bind to BSA. This phenomenon shows that binding of C_{14} mimBr to BSA at concentrations near the CMC depends on hydrophobic interactions which are dependent on temperature [22]. The values of γ_{CMC} without BSA are lower than that with BSA, which shows the existence of C_{14} mimBr/BSA complexes at the air/water interface and that their surface activity is not superior to C_{14} mimBr.

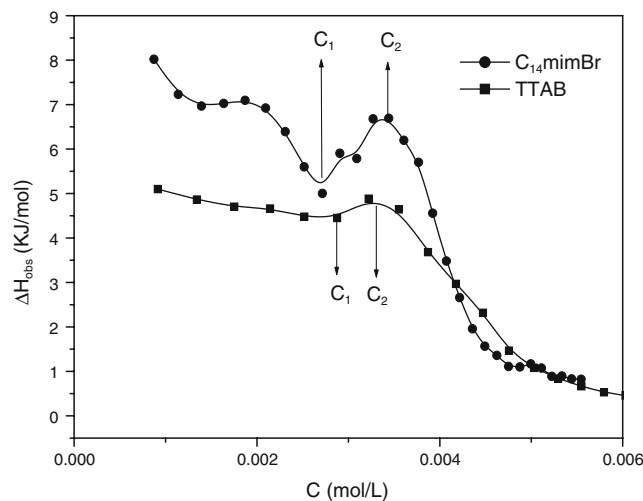
Interaction enthalpy between C_{14} mimBr and BSA

Microcalorimetry can be used to offer a direct and precise determination of the enthalpy change between macromolecules and ligand. As the literature about protein/ligand interactions reports [23], control experiments of binding properties of protein with surfactant by isothermal titration microcalorimetry include the titration of surfactant into water, water into protein and dilution of water. The last two controls resulted in small changes and were not considered. Figure 3 shows the enthalpy of titration of C_{14} mimBr into water and TTAB into water which are control experiments for the C_{14} mimBr/BSA interaction and TTAB/BSA interaction.

Endothermic enthalpy changes resulting from injection of surfactant solutions into 5×10^{-5} -mol/L BSA solution were measured (subtracting the control experiment; Fig. 4). The enthalpy changes in the presence of BSA become more endothermic which indicate that there are interactions between the surfactants and BSA besides the demicellization of the surfactants. The general shape of the enthalpy vs. surfactant concentration for the C_{14} mimBr/BSA system is similar to that of the TTAB/BSA system. The two curves can be both divided into three different regions. In region I (when the concentration of surfactant is below C_1), the enthalpy decreases with injection of surfactant because C_{14} mimBr or TTAB monomers bind to specific sites on the

**Fig. 3** Enthalpy plots for C_{14} mimBr and TTAB micellization at 25 °C

BSA surface [24, 25]. It is proposed that the cationic surfactant head groups bind to anionic protein groups, while the non-polar surfactant tails bind to nearby hydrophobic patches on the protein surface [4]. At the beginning, there is an electrostatic repulsion between BSA molecules which is large enough to prevent them from associating. When surfactant is continuously added to the BSA solution, it reduces the net negative charge on the BSA [15]. In region II (when the concentration of surfactant is between C_1 and C_2), there is an increase in enthalpy from a minimum to a maximum with increasing surfactant concentration. The increment of C_{14} mimBr is especially significant. In region II, surfactant molecules promote BSA denaturation by binding to them. The maximum in the enthalpy vs. surfactant concentration may be due to BSA unfolding [5]. As BSA molecules bind more surfactants, their net electrical charge initially tends towards zero.

**Fig. 4** Enthalpy plots of C_{14} mimBr/BSA and TTAB/BSA at 25 °C

So, there is little electrostatic repulsion among the surfactant/BSA complexes, and the complexes aggregate. However, as the surfactant concentrations further increase, BSA can bind more cationic surfactant molecules, and their net charge becomes increasingly positive. Above a certain surfactant concentration, the net positive charge on the surfactant/BSA complexes can be sufficiently large to oppose aggregation and so the aggregates dissociate [15]. The enthalpy in region II may, therefore, be due to a combination of surfactant-to-BSA interactions and BSA aggregation/dissociation. At the beginning of region III (where the concentration of surfactant is above C_2), it is postulated that the surfactant concentrations exceed the CMC and so the surfactants begin to form micelles. The evidence for this assertion is that there is an appreciable decrease in enthalpy, which is similar to that observed when micelles form in the absence of protein (Fig. 3). It is obvious that the enthalpy value of C_{14} mimBr/BSA system is higher than that of TTAB/BSA system, which indicates that the interaction between C_{14} mimBr and BSA is more intense. As discussed in surface tension part, C_{14} mimBr binding to BSA at concentrations near the CAC depends mainly on electrostatic interactions and at concentrations near the CMC depends mainly on hydrophobic interactions. So the differences between C_{14} mimBr/BSA and TTAB/BSA in enthalpy value are caused by the molecular structure differences between C_{14} mimBr and TTAB. As reported, C_{14} mimBr has the potency of hydrogen bond formation among imidazolium head groups, which is lacking in TTAB [26]. This means that when C_{14} mimBr aqueous solution is titrated into BSA aqueous, the hydrogen bond is damaged firstly and the C_{14} mimBr molecules bind to BSA then. The enthalpy value of C_{14} mimBr/BSA in Fig. 3 includes the enthalpy values of the two processes.

Secondary structure content of BSA

Far-UV CD measurements can calculate the secondary structure of proteins. Figure 5 shows far-UV CD spectra of 5×10^{-5} mol/L BSA in the presence of increasing C_{14} mimBr concentrations. Since the surfactant molecules do not present any CD signal in the spectral range from 200 nm to 260 nm, the observed CD results are due to BSA alone. When the concentration of C_{14} mimBr ranges from 3×10^{-5} mol/L to 1×10^{-3} mol/L, the far-UV CD spectra curves are almost superimposable, which indicates that the α -helix structure has no change. This phenomenon can be explained by the fact that the surfactant molecules bind specifically to high-energy sites of BSA and stabilize the secondary structure of BSA by cross-linking [5]. Low concentrations of C_{14} mimBr induce a more compact state of BSA [1]. As the concentration of C_{14} mimBr increases beyond 1×10^{-3} mol/L, the negative bands at 222 nm are

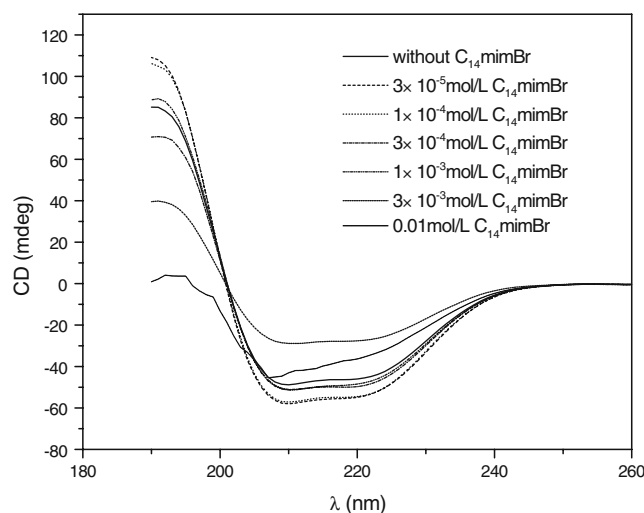


Fig. 5 Far-UV CD of C_{14} mimBr/BSA at 25 °C

lost. When the concentration of C_{14} mimBr is higher than 3×10^{-3} mol/L (above the CMC), the secondary structure is totally disrupted. The surfactant molecules induce the unfolding of BSA. This result is consistent with that of the isothermal titration microcalorimetry.

The contents of α -helical and random coil are listed in Table 2. The percentages of α -helical and random coil are essentially unchanged as the concentration of C_{14} mimBr ranges from 3×10^{-5} mol/L to 1×10^{-3} mol/L. This result emphasizes that low concentrations of C_{14} mimBr stabilize the secondary structure of BSA. The percentage of α -helix decreases and the percentage of random coil increases rapidly when the concentration of C_{14} mimBr increases to 1×10^{-2} mol/L. This indicates unfolding of BSA due to its combination with C_{14} mimBr.

Polarity of the microenvironment around specific amino acid residues

Fluorescence was used to monitor the changes on the tertiary structure of BSA induced by the interaction with C_{14} mimBr. BSA has three intrinsic fluorophores, viz. Trp residues, Tyr residues, and phenylalanine (Phe) residues. Trp residues are abundant in BSA and show an emission peak at 348 nm. Tyr residues have an emission peak at 303 nm and can be exposed to solvent induced by C_{14} mimBr. The quantum yield of Phe residues in BSA is rather low [27], so, the emission from this residue can be ignored.

Steady-state fluorescence spectra

Figure 6 shows the steady fluorescence spectrum of 5×10^{-5} mol/L BSA. When the concentration of C_{14} mimBr is below 3×10^{-3} mol/L (slightly below the CMC), addition of C_{14} mimBr to the BSA solution leads to a decrease in the

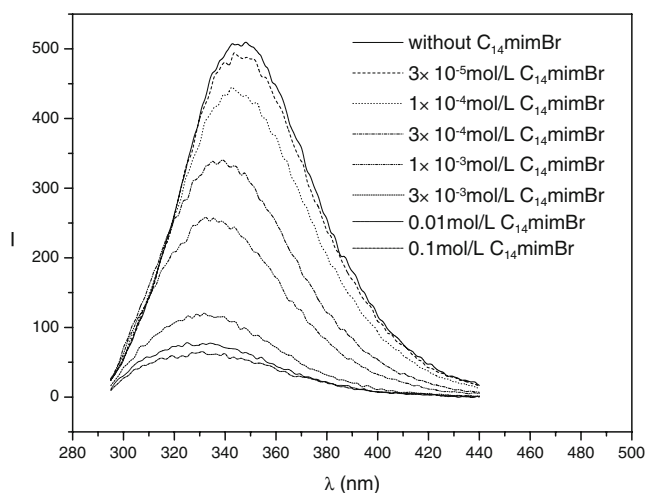
Table 2 Contents of α -helical and random coil on C_{14} mimBr concentrations

Concentration of C_{14} mimBr (mol/L)	3×10^{-5}	1×10^{-4}	3×10^{-4}	1×10^{-3}	3×10^{-3}	0.01
α -helical (%)	28.9	28.5	28.9	28.7	24.7	19.5
Random coil (%)	30.5	30.2	30.2	30.1	30.9	33.3

fluorescence intensity and this is accompanied by a hypsochromic shift of the maximum emission peak. The fluorescence intensity decreases from 509 (without C_{14} mimBr) to 120 (3×10^{-3} mol/L C_{14} mimBr), and the maximum emission peak shifts from 348 to 331 nm. This shift suggests that the amino acid residues are exposed to a more hydrophobic microenvironment which is attributed to the burial of Trp residues [1]. This phenomenon suggests the formation of C_{14} mimBr/BSA complexes. When the concentration of C_{14} mimBr is above 3×10^{-3} mol/L, the fluorescence intensity and the maximum emission peak are nearly unchanged due to the denaturation of BSA in the presence of a high concentration of C_{14} mimBr. Both the isothermal titration microcalorimetry and far-UV CD spectra results indicate that when the C_{14} mimBr concentration exceeds 3×10^{-3} mol/L, BSA unfolds and denatures.

Synchronous fluorescence spectra

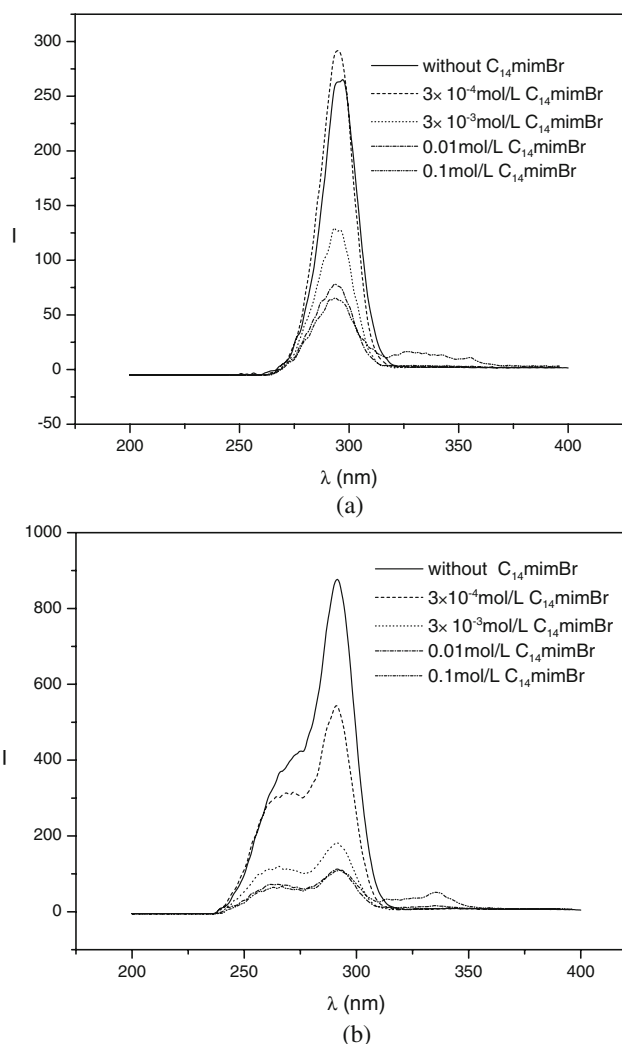
Synchronous fluorescence spectra can offer several advantages: spectral simplification, spectral bandwidth reduction, and avoiding different perturbing effects [28]. Synchronous fluorescence spectra of BSA at a concentration of 5×10^{-5} mol/L are shown in Fig. 7. The fluorescence intensity of BSA for $\Delta\lambda=60$ nm is higher than that for $\Delta\lambda=20$ nm. So, the intrinsic fluorescence of BSA can be almost completely attributed to the Trp residues [29]. Figure 7a reveals that the fluorescence intensity of the Trp residues decreases from 874 to 182 rapidly with an increasing concentration of C_{14} mimBr (from 0 to 3×10^{-3} mol/L). But no significant change in wavelength is observed, which

**Fig. 6** Steady-state fluorescence of C_{14} mimBr/BSA at 25 °C

suggests that the interaction of C_{14} mimBr with BSA does not affect the microenvironment of the Trp residues [30]. When the concentration of C_{14} mimBr is above 3×10^{-3} mol/L, the fluorescence intensity changes little which indicates the denaturation of BSA as in the steady-state fluorescence experiments.

Conclusions

The present study reveals that with a surface active imidazolium IL, C_{14} mimBr can bind to BSA. The combination occurs by electrostatic interaction at low C_{14} mimBr

**Fig. 7** Synchronous fluorescence of C_{14} mimBr/BSA at 25 °C. **a** $\Delta\lambda=20$ nm. **b** $\Delta\lambda=60$ nm

concentration and by hydrophobic interaction at high $C_{14}\text{mimBr}$ concentration. $C_{14}\text{mimBr}$ stabilizes the secondary structure of BSA at low concentration (below the CMC) but destroys the secondary structure of BSA at high concentration (above the CMC). The destruction of the secondary structure leads to unfolding of the BSA structure and BSA denaturation ultimately. The secondary structure changes of BSA are due to the interactions of $C_{14}\text{mimBr}$ molecules and amino acid residues. Compared with traditional cationic surfactants, $C_{14}\text{mimBr}$ is superior in both protection and destruction of BSA, depending on the concentration. This study shows the potential importance of interactions between $C_{14}\text{mimBr}$ and BSA.

Acknowledgments This work was supported by the Natural Science Foundation of China (20773081), the Natural Science Foundation of Shandong Province of China (Z2007B03), and the Doctoral Fund of the Ministry of Education of China (New Teachers Fund) (070422047). The authors thank Dr. Pamela Holt for editing the manuscript.

References

- Parker W, Song PS (1992) *Biophys J* 61:1435
- Singh SK, Kishore NJ (2006) *J Phys Chem B* 110:9728
- Ananthapadmanabhan KP (1993) Protein-surfactant interactions. In: Goddard ED, Ananthapadmanabhan KP (eds) *Interactions of surfactants with polymers and proteins*. Boca Raton, CRC Press, New York, pp 319–366
- Jones MN, Chapman MN (1995) In: Jones MN, Chapman MN (eds) *Micelles, monolayers and biomembranes*. Wiley, New York, p 252
- Li YJ, Wang XY, Wang YL (2006) *J Phys Chem B* 110:8499
- Kelly D, McClements DJ (2003) *Food Hydrocoll* 17:73
- Cooper A (1999) *Curr Opin Chem Biol* 3:557
- Ghosh S, Banerjee AA (2002) *Biomacromolecules* 3:9
- Gharibi H, Javadian S, Hashemianzadeh M (2004) *Colloid Surf A* 232:77
- Ruso JM, González-Pérez A, Prieto G, Sarmiento F (2003) *Int J Biol Macromol* 33:67
- Stenstam A, Montalvo G, Grillo I, Gradzielski M (2003) *J Phys Chem B* 107:12331
- Trynda-Lemiesz L (2004) *Bioorg Med Chem* 12:3269
- Barbosa S, Taboada P, Attwood D, Mosquera V (2003) *Langmuir* 19:10200
- Hu YJ, Liu Y, Pi ZB, Qu SS (2005) *Bioorg Med Chem* 13:6609
- Magdassi S, Vinetsky Y, Relkin P (1996) *Colloid Surf B* 6:353
- Dong B, Li N, Zheng LQ, Yu L, Inoue T (2007) *Langmuir* 23:4178
- Drapper NR, Smith H (1968) In: Drapper NR, Smith H (eds) *Applied regression analysis*. Wiley, New York, p 73
- Magzoub M, Kilk K, Eriksson LEG, Langel Ü, Gräslund A (2001) *Biochim Biophys Acta Biomembr* 1512:77
- Fuller CW, Miller JN (1979) *Proc Anal Div Chem Soc* 16:199
- Tang JH, Luan F, Chen XG (2006) *Bioorg Med Chem* 14:3210
- Rosen MJ (1989) In: Rosen MJ (ed) *Surfactants and interfacial phenomena*. Wiley, New York, p 115
- Zhao GX (1984) Structure and characteristic of surfactant. In: Zhao GX (ed) *Surfactant physical chemistry*. Press of Beijing University, Beijing, p 724
- O'Brien R, Ladbury JE, Chowdhry BZ (2001) In: Harding SE, Chowdhry BZ (eds) *Protein–ligand interactions: Hydrodynamics and calorimetry*. Oxford University Press, Oxford, pp 263–286
- Oakes J (1973) *Eur J Biochem* 36:553
- Oakes J, Coff MC (1973) *Eur J Biochem* 36:559
- Inoue T, Ebina H, Dong B, Zheng LQ (2007) *J Colloid Interface Sci* 314:236
- Liu WG, Yao KD, Wang GC, Li HX (2000) *Polymer* 41:7589
- Wang F, Yang JH, Wu X, Sun CX, Liu SF, Guo CY, Jia Z (2005) *Chem Phys Lett* 409:14
- Wu D, Xu GY, Sun YH, Zhang HX, Mao HZ, Feng YJ (2007) *Biomacromolecules* 8:708
- Anbzhagan V, Renganathan R (2008) *J Lumin* 128:1454